Straightforward strategy for selecting and tuning substrates for two-dimensional material epitaxy

Chao He,[1] Shaogang Xu,[1] Changchun He,[1] Xingxing Dong,[1] Feini Yan,[1] Xiangting Hu,[1] and Hu Xu[1,2,3,*]

[1]*Department of Physics, Southern University of Science and Technology, Shenzhen 518055, People's Republic of China*

[2]*Shenzhen Key Laboratory of Advanced Quantum Functional Materials and Devices, Southern University of Science and Technology, Shenzhen 518055, People's Republic of China*

[3]*Guangdong Provincial Key Laboratory of Computational Science and Material Design, Southern University of Science and Technology. Shenzhen 518055, People's Republic of China*

(Received 21 April 2022; accepted 16 June 2022; published 29 June 2022)

Wafer-scale two-dimensional (2D) materials grown directly on substrates via epitaxy methods are desired for building high-performance electronic devices. Up to now, the selection of the appropriate substrates has been dominated by trial and error, which has greatly hindered the mass production of 2D materials for device applications. In this paper, based on the evolutionary trend of the formation energy during growth, we propose that the epitaxy of monoelemental 2D materials on metal substrates can be classified into three types, and only the third type with a significant energy benefit has the opportunity to grow into large-scale 2D monolayers. By extensive first-principles calculations, we find that this concept can coincide well with experimental reports when the energy threshold is set to 0.6 eV/atom, which provides a straightforward way to evaluate interlayer interactions between substrates and adsorbates. Furthermore, taking the growth of blue phosphorene (blue-P) on Ag(111) as an example, a heterogeneous epitaxial strategy to achieve a transition in growth type by surface alloying is proposed. We verify the feasibility of this strategy and investigate the nucleation process of blue-P on the Ag_2Sb surface alloy. Our findings provide a valid path for substrate selection and tuning, and we believe that this general strategy will stimulate the development of the large-scale synthesis of 2D materials.

DOI: 10.1103/PhysRevMaterials.6.064011

I. INTRODUCTION

Inspired by the extraordinary properties of graphene [1], two-dimensional (2D) materials have sparked everlasting research interests for their promising applications in future electronic devices. Besides graphene, the emergence of other 2D materials, such as hexagonal boron nitride (h-BN) [2,3], transition metal dichalcogenides [4], silicene [5,6], borophene [7,8], and black phosphorene [9,10], have also been produced and studied. However, the synthesis of wafer-scale 2D materials is the first critical step for industrial applications and currently remains a significant challenge. Top-down isolation of layered bulk crystals using mechanical/liquid exfoliation techniques often generates nanosheets with small and uncontrollable sizes, and this technique is unable to fabricate 2D materials that lack corresponding layered bulk counterparts [e.g., blue phosphorene (blue-P) [11]]. As the most promising method for synthesizing wafer-level 2D materials, the bottom-up epitaxial growth of 2D materials on appropriate substrates has drawn great attention in the past few years [12]. For example, the epitaxial growth of graphene and h-BN on Cu(111) [13,14], Ag(111) [15,16], and Au(111) [17,18] surfaces has been extensively explored. Among all reported growth cases, the epitaxy of monoelemental 2D materials on various metal substrates provides suitable templates for exploring growth mechanisms [12,19].

Unlike the classical epitaxial theory, interfacial effects become more relevant when the film thickness is reduced to monolayers, which usually leads to substrate selection becoming extremely important [20,21]. For instance, coinage metals with distinct chemical reactivity are the most widely used substrates for monoelemental 2D material epitaxy. However, only cluster-structural blue-P has been fabricated on Ag(111) at a substrate temperature of 420 K [22], while only metal phosphides have been formed on both Au(111) [23] and Cu(111) [24]. Likewise, silicene has only been successfully grown on Ag(111) [5] due to its moderate interfacial interaction, and the ordered Cu_2Si [25] and Au-Si [26] alloys have been obtained on Cu(111) and Au(111), respectively. To sum up, too strong interactions between substrates and precursors usually limit the surface aggregation of adsorbates, while too weak interactions prefer to form 3D islands. Several theoretical works have been presented to explore the interlayer interactions between metal substrates and adsorbates during epitaxial growth [21,27], but a straightforward and conceptually intuitive approach is still missing.

In this paper, based on the evolutionary trend of the formation energy during growth, we propose a straightforward classification to evaluate the interaction between metal substrates and adsorbates. Using extensive first-principles calculations, we provide a specific energy criterion of 0.6 eV/atom and confirm that the experimentally reported growth cases indeed satisfy our prediction. In addition, using blue-P growth on Ag(111) as an example, we propose to modulate interlayer interactions by surface alloying to achieve a transition in growth type. To gain deeper insights, we verify

*xuh@sustech.edu.cn

the feasibility of this strategy and confirm the suitable charge transfer of blue-P on the Ag_2Sb surface. Our results provide useful insights into the synthesis of high-quality 2D materials on suitable substrates.

II. COMPUTATIONAL METHODS

All the *ab initio* calculations are performed using the Vienna *ab initio* simulation package (VASP) [28,29] and based on the projector augmented-wave approach (PAW) with the Perdew-Burke-Ernzerhof (PBE) generalized gradient approximation [30]. The density functional theory (DFT-D3) [31] method is employed to account for the van der Waals (vdW) interaction. A kinetic energy cutoff of 450 eV and a convergence criteria of 10^{-5} eV are used in all the calculations. The 2D Brillouin zones are sampled by uniform k-point meshes with a spacing of about 0.03/Å. A conjugate-gradient algorithm is used to relax the ions until the force is less than 0.02 eV/Å. The substrate surfaces are modeled as slabs consisting of five layers, and the thickness of the vacuum layer is 15 Å. The bottom layers of substrates are fixed and the other four layers are further relaxed during the geometry relaxation. The charge density difference and slices are plotted with the VESTA software package [32]. We performed lattice matching by the package of structures of alloy generation and recognition (SAGAR) [33,34].

III. RESULTS AND DISCUSSION

The stability of adsorbates on metal surfaces has been widely evaluated by the formation energy (E_{form}) [35]. E_{form} is defined as

$$E_{\text{form}} = \frac{E_{\text{tot}} - E_{\text{sub}} - N \times E_a}{N}, \tag{1}$$

where E_{tot} and E_{sub} are energies of a whole system and a substrate, respectively. E_a is the energy of one adsorbate in its stable bulk phase, and N is the number of adsorbates on the substrate. We further define $\Delta E = E_{\text{form}}^{\text{atom}} - E_{\text{form}}^{\text{ml}}$ to describe the interaction difference between the formation energies of an individual adsorbate ($E_{\text{form}}^{\text{atom}}$) and the corresponding monolayer ($E_{\text{form}}^{\text{ml}}$) adsorbed on substrates.

Without loss of generality, we can categorize the epitaxy of monoelemental 2D materials on various metal substrates into three types, depending on the evolutionary trend of E_{form}. As shown in Fig. 1(c), type C represents that as the size increases, from an individual atom to a discrete cluster and finally to a desired monolayer, the decline trend of E_{form} is very obvious. For type C, a large ΔE is sufficient to support the large-scale growth of 2D materials on substrates. For type A shown in Fig. 1(a), E_{form} increases with size, indicating extremely strong interactions between the substrates and adsorbates, which is generally difficult to obtain ideal 2D materials and usually yields alloys. In Fig. 1(b), for type B, although their ΔE is larger than 0, the smaller energy gain means that there remains a relatively strong interlayer interaction, and the surface aggregation behavior of adsorbates is still limited. Besides alloys, type B also holds promise for small clusters.

To verify our viewpoint, we calculated ΔE of eight monoelemental 2D materials (i.e., borophene, graphene, silicene, germanene, stanene, phosphorene, antimonene, and bismuthene) on commonly used metal substrates (see the Supplemental Material for details [36]). As shown in Fig. 2, for 2D materials that have been successfully prepared through numerous independent experiments (see the green panel in Fig. 2) [5,8,13,15,17,37–40], we find that ΔE is over 0.6 eV/atom, corresponding exactly to the expected type C, which can be attributed to the strong intralayer interactions of borophene, graphene, and silicene with the corresponding cohesive energies of 7.37, 5.81, and 4.63 eV/atom [27], respectively. However, the interlayer interaction between adsorbates and substrates is variable and can be modulated by substrate selection. For example, graphene has been successfully synthesized on Cu(111) [13], Ag(111) [15], Au(111) [17], and Pt(111) [37], and all ΔE are greater than the threshold value of 0.6 eV/atom. For borophene, various boron monolayers have been experimentally reported on Al(111), Ag(111), and Au(111), while an experimental report of borophene on Pt(111) is lacking because ΔE is less than 0.6 eV/atom (see all ΔE in Table S1). Among all coinage metals, silicene can only grow on Ag(111) [5] with ΔE of 0.677 eV/atom, which is above the threshold value of 0.6 eV/atom.

More convincingly, for surface alloys [see the yellow and red panels in Fig. 2, P-Au(111), and P-Cu(111)] [23,25,41–49] and clusters [P-Ag(111) [22]] in experiments, we are indeed able to divide them into two types. Specifically, when ΔE is over 0 and below 0.6 eV/atom, this corresponds to type B. Here, ΔE for P-Ag(111) is 0.363 eV/atom, which does not reach the threshold value of 0.6 eV/atom. Therefore, only the cluster-structural blue-P [22] or quasi-1D phosphorene chains [50] were fabricated, while Si-Cu(111) [25], Ge-Ag(111) [41], and Sn-Ag(111) [42] were all reported to form surface alloys. As expected, for type A with ΔE less than 0, most reported results are alloyed structures. Ordered alloys such as Cu_2Sb [48], Cu_2Sn [51], Cu_2Bi [47], and Ag_2Sb [52] have been prepared on Cu(111) and Ag(111), respectively. Furthermore, for more chemically active metal surfaces such as Pt(111) and Au(111), the alloying of Si-Au(111) [26], Sn-Au(111) [42], Sn-Pt(111) [53], Sb-Pt(111) [54], and the formation of a porous Au-P network [23] on P-Au(111) have

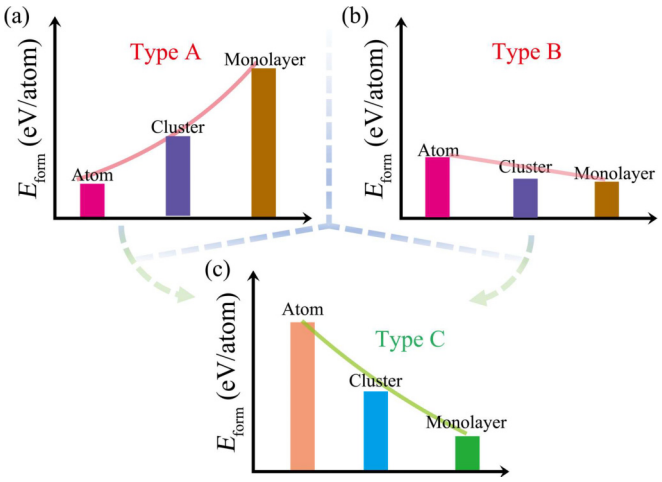

FIG. 1. Schematic diagram of the trend of E_{form} for growing monoelemental 2D materials on potential metal substrates. (a) Type A. (b) Type B. (c) Type C.

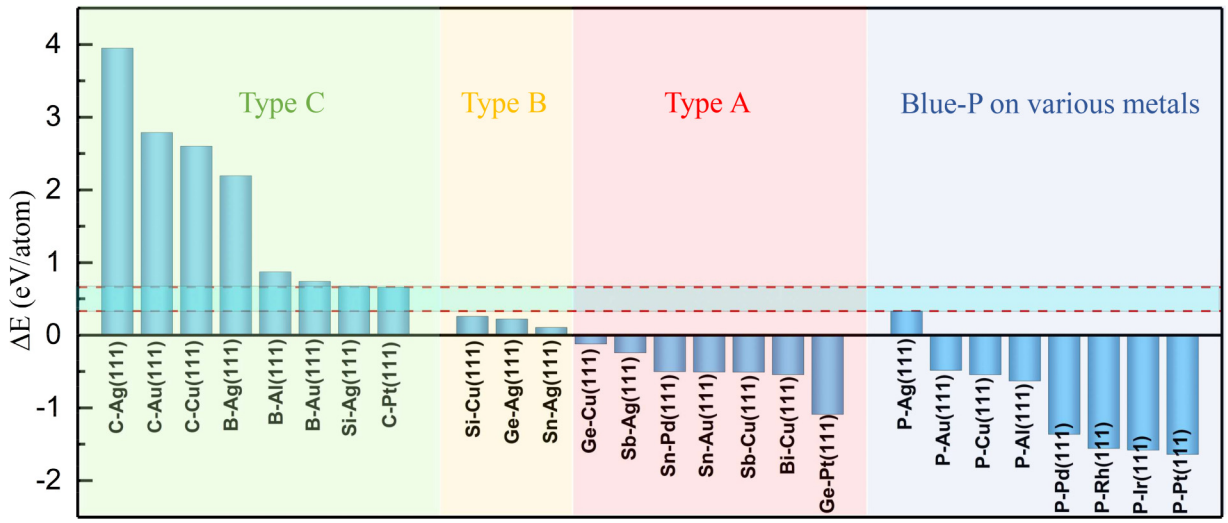

FIG. 2. ΔE of monoelemental 2D materials on fcc metal (111) surfaces. Blue columns represent the energy difference ΔE between an individual adsorbate and the corresponding monolayer on metal substrates.

been reported experimentally, and ΔE for these cases are well below zero, also indicating a stronger interlayer interplay between these substrates and adsorbates.

For later discussion, we also performed calculations for the rarely reported growth of blue-P on Al(111), Pt(111), Pd(111), Rh(111), and Ir(111), and we found that ΔE for all these configurations are below zero. These results are also consistent with some recent theoretical works [24,55–57]. Collecting all the results in Fig. 2, no data distribution is found in the energy interval 0.4–0.6 eV/atom. Herein, we emphasize that experimental reports that remain highly controversial, such as Ge-Al (111) [58], Ge-Au (111) [59], and Ge-Pt (111) [60], were not discussed much in this work. For these cases, we infer that it is highly likely that alloys appear, which requires further experimental verification. It is also worth noting that although experimental synthesis processes are influenced by many variables such as substrate selection, interfacial chemistry, temperature, and deposition rates, substrate selection is particularly important as it can decrease the nucleation energy of a given target, especially the metastable phase in vacuum [61].

After clarifying the correlation between interlayer interactions and ΔE, it is natural to artificially modulate the interaction between adsorbates and substrates until the energy threshold is satisfied. Introducing buffer layers by means of surface alloying or interfacial intercalation is one effective method to modulate the interaction strength from type A or type B to type C, enabling suitable substrates for the self-assembled epitaxy of 2D materials. Surface alloys may also allow the growth of ordered surface structures, which are categorized into homogeneous epitaxy and heterogeneous epitaxy modes. For homogeneous epitaxy, stanene/Pd_2Sn [49], stanene/Ag_2Sn [42], antimonene/Cu_2Sb [62], and antimonene/Ag_2Sb [52] have been experimentally reported. Our results show that ΔE rise to 1.118, 0.605, 1.386, and 1.060 eV/atom after substrate alloying compared to ΔE of −0.501, 0.107, −0.608, and −0.240 eV/atom for Sn-Pt(111), Sn-Ag(111), Sb-Cu(111), and Sb-Ag(111), respectively. These results still meet our energy threshold and achieve the transition from type A or type B to type C. Therefore, suitable surface alloys can weaken the vertical interaction between metal substrates and adsorbates, allowing 2D materials to grow laterally in a self-assembled manner. For heteroepitaxy, few 2D materials are reported, and there is still much room for exploration.

To apply this strategy to practical problems of growing 2D materials, we have performed theoretical calculations using the growth of blue-P as an example. Although many theoretical and experimental works were suggested to prepare blue-P on Au(111) [63–65], we have confirmed the Au-P network rather than blue-P on Au(111) [23]. Buffer layers were introduced by intercalation of Si on Au(111) [66] and oxidation of Cu(111) [67], but the structural characteristics of buffer layers are unclear, which significantly hinders the growth of high-qualified blue-P.

In the following, we explored the feasibility of growing blue-P on the Ag_2Sb surface alloy. Compared with other commonly used metal substrates, the interaction between Ag(111) and P element is relatively weak, making the alloying of the Ag(111) surface most likely to synthesize monolayer blue-P. It is worth mentioning that the interaction strength between P and transition metals can be explained by the d-band center theory [68]. Moreover, Ag_2Sb belongs to a class of typical surface alloys Ag_2M (M = Sb, Sn, Pb, and Bi) with C_{3v} symmetry [41,43], which meets the symmetry requirements for blue-P growth [20], as shown in Figs. 3(a) and 3(b). E_{form} for an individual P atom, hexagonal P_{24} cluster, and blue-P monolayer on the Ag(111) surface are 0.126, −0.196, and −0.237 eV/atom, respectively, as shown in Fig. 3(c). Although ΔE (0.363 eV/atom) for Ag(111) is smaller than the threshold value of 0.6 eV/atom, it is larger than those on Pt(111) and Au(111), leading to the formation of the cluster-structural blue-P. On the Ag_2Sb surface alloy, the corresponding E_{form} increase to 1.036, 0.060, and −0.035 eV/atom, respectively, as shown in Fig. 3(d). As a result, ΔE increases to 1.071 eV/atom, which is markedly larger than the threshold value

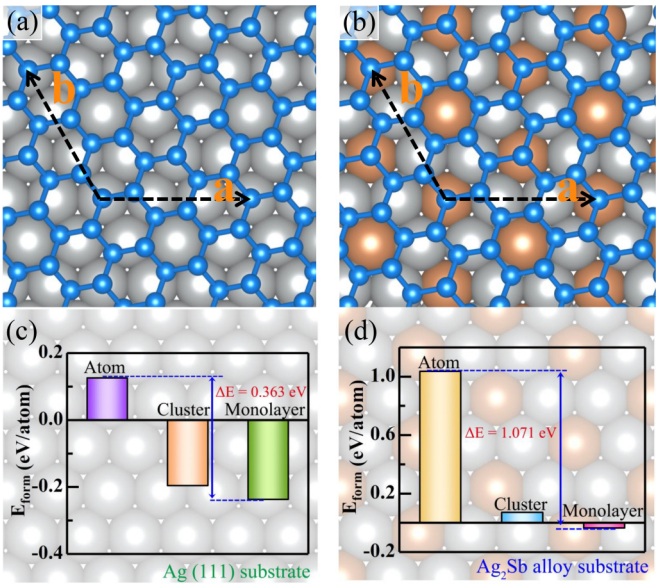

FIG. 3. (a), (b) Top views of blue-P on Ag(111) and Ag_2Sb, respectively. Formation energies of single atom, cluster (P_{24}), and blue-P monolayer on (c) Ag(111) and (d) Ag_2Sb, respectively. The blue, gray, and brown spheres represent P, Ag, and Sb atoms, respectively.

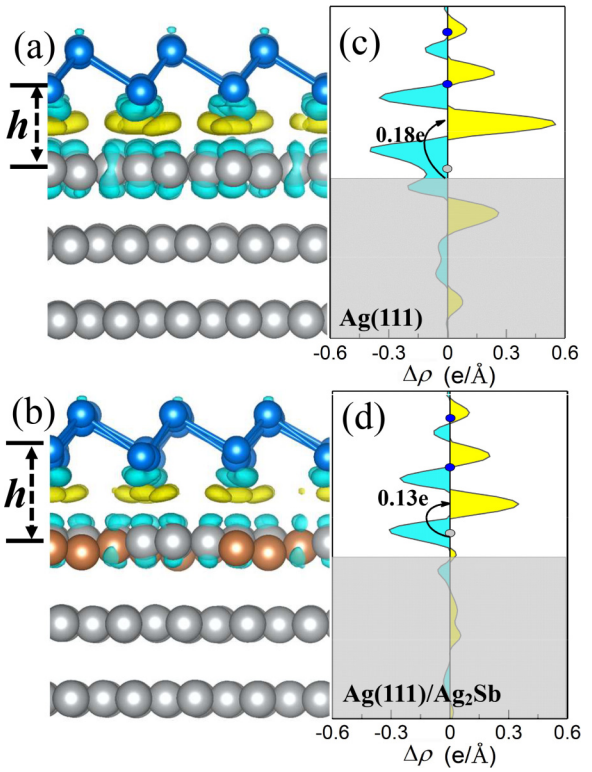

FIG. 4. Charge density difference plots of blue-P on (a) Ag(111) and (b) Ag_2Sb/Ag(111). The isosurface is 0.03 e/bohr^3. Averaged plane electron density difference $\Delta\rho$ along the direction perpendicular to the interface for (c) Ag(111) and (d) Ag_2Sb/Ag(111). The yellow and blue colors represent the accumulation and depletion of electrons, respectively.

of 0.6 eV/atom to grow 2D monolayers. Furthermore, two P atoms on the Ag_2Sb surface tend to bond together with an energy reduction of 1.028 eV, which also indicates that the P atoms prefer to aggregate. Therefore, Ag_2Sb is an ideal substrate for the epitaxy of blue-P monolayer.

To gain deeper insights into the interactions of blue-P with pure metal and alloy substrates, we compare the charge density difference of monolayer blue-P on Ag(111) and Ag_2Sb, as shown in Figs. 4(a) and 4(b). It can be clearly seen that the amount of charge transfer between Ag(111) and monolayer blue-P is large, which indicates that the interlayer interaction at the interface is strong, while it is greatly decreased for monolayer blue-P on Ag_2Sb. With the decreased charge transfer, the vertical distance (h) between blue-P and substrates is increased from 2.38 Å for Ag(111) to 2.61 Å for Ag_2Sb. The h of blue-P/Ag(111) is close to the sum of covalent radii of Ag (1.28 Å) and P (1.11 Å), i.e., 2.39 Å, while the sum of the covalent radii of Sb (1.40 Å) and P, i.e., 2.51 Å, is smaller than h for Ag_2Sb, which indicates that the chemical binding between blue-P and Ag_2Sb is weakened. Furthermore, Figs. 4(c) and 4(d) show the charge transfer along the direction perpendicular to the interface, and it is found that the charge accumulation is in the region between blue-P and substrates. For blue-P/Ag(111), 0.18 electrons are transferred from the topmost Ag surface to the interface of blue-P/Ag(111), while the amount of charge transfer is 0.13 electrons for blue-P/Ag_2Sb/Ag(111), indicating a stronger interaction between the Ag(111) surface and monolayer blue-P. If we choose the binding energy of 0.03 eV/Å^2 as the criterion for the exfoliation of 2D materials [69], the binding energy for monolayer blue-P on the Ag_2Sb surface is 0.028 eV/Å^2, showing the possibility of exfoliating freestanding blue-P in experiments. By comparison, the binding energy between blue-P and Ag(111) is 0.065 eV/Å^2, which is much stronger that it may prevent it from being exfoliated from the Ag(111) substrate.

To examine the nucleation mechanism in the early stages of growth, P_N clusters up to $N = 24$ on the Ag_2Sb surface were considered in the Supplemental Material [36]. Until the P_{24} island appears, $E_{\text{form}}^{\text{cluster}} - E_{\text{form}}^{\text{monolayer}}$ is 0.095 eV/atom, which has a greater energy advantage than that on Ag(111) (0.041 eV/atom) to continue self-assembly growth. With increasing P coverage, P-P interactions become more important and gradually become the major determinant of the surface structure. Thus, the P-P interaction drives P atoms to adopt their blue-P lattice structure, giving rise to a commensurate monolayer. To further examine the thermal stability of blue-P on the Ag_2Sb surface alloy, we performed molecular dynamics simulations at 300 K in Fig. S2, and the blue-P monolayer retains the structure. In addition, we extend our studies to other Ag_2M surface alloys and dig out two other candidates that could be applied to blue-P growth, as listed in Table S3. Among them, Ag_2Bi possesses a much larger ΔE (1.212 eV/atom) and Ag_2Sn has a slightly smaller ΔE (0.640 eV/atom).

IV. CONCLUSIONS

In summary, based on the evolutionary trend of the formation energy during growth, we have proposed a strategy

to intuitively evaluate the strength of interlayer interactions. By extensive first-principles calculations combined with numerous experimental reports, we have determined an energy threshold of 0.6 eV/atom for 2D material epitaxy. Furthermore, taking the growth of blue-P on Ag(111) as an example, we have proposed that the surface alloy serves as a buffer layer for growing blue-P in a heterogeneous way, enabling a transition in growth type. Combined with comparative formation energy, charge density difference, and bonding analysis, we have verified the feasibility of this scheme and demonstrated the nucleation and growth process of blue-P on the Ag_2Sb surface alloy in the early stages. These theoretical results help prescribe the fundamental principle for the choice of substrates to grow 2D materials. Moreover, our work also delivers some valuable insights into the epitaxy of multielemental 2D materials or epitaxy using insulator substrates.

ACKNOWLEDGMENT

This work is supported by the National Natural Science Foundation of China (Grant No. 11974160), the Science, Technology, and Innovation Commission of Shenzhen Municipality (Grants No. RCYX20200714114523069 and No. ZDSYS20190902092905285), the fund of the Guangdong Provincial Key Laboratory of Computational Science and Material Design (No. 2019B030301001), and the Center for Computational Science and Engineering at Southern University of Science and Technology.

[1] K. S. Novoselov, A. K. Geim, S. V. Morozov, D.-e. Jiang, Y. Zhang, S. V. Dubonos, I. V. Grigorieva, and A. A. Firsov, Science **306**, 666 (2004).
[2] L. Song, L. Ci, H. Lu, P. B. Sorokin, C. Jin, J. Ni, A. G. Kvashnin, D. G. Kvashnin, J. Lou, B. I. Yakobson *et al.*, Nano Lett. **10**, 3209 (2010).
[3] R. Y. Tay, M. H. Griep, G. Mallick, S. H. Tsang, R. S. Singh, T. Tumlin, E. H. T. Teo, and S. P. Karna, Nano Lett. **14**, 839 (2014).
[4] Q. H. Wang, K. Kalantar-Zadeh, A. Kis, J. N. Coleman, and M. S. Strano, Nat. Nanotechnol. **7**, 699 (2012).
[5] B. Feng, Z. Ding, S. Meng, Y. Yao, X. He, P. Cheng, L. Chen, and K. Wu, Nano Lett. **12**, 3507 (2012).
[6] A. Fleurence, R. Friedlein, T. Ozaki, H. Kawai, Y. Wang, and Y. Yamada-Takamura, Phys. Rev. Lett. **108**, 245501 (2012).
[7] A. J. Mannix, X.-F. Zhou, B. Kiraly, J. D. Wood, D. Alducin, B. D. Myers, X. Liu, B. L. Fisher, U. Santiago, J. R. Guest *et al.*, Science **350**, 1513 (2015).
[8] B. Feng, J. Zhang, Q. Zhong, W. Li, S. Li, H. Li, P. Cheng, S. Meng, L. Chen, and K. Wu, Nat. Chem. **8**, 563 (2016).
[9] L. Li, Y. Yu, G. J. Ye, Q. Ge, X. Ou, H. Wu, D. Feng, X. H. Chen, and Y. Zhang, Nat. Nanotechnol. **9**, 372 (2014).
[10] H. Liu, A. T. Neal, Z. Zhu, Z. Luo, X. Xu, D. Tománek, and P. D. Ye, ACS Nano **8**, 4033 (2014).
[11] Z. Zhu and D. Tománek, Phys. Rev. Lett. **112**, 176802 (2014).
[12] D. Zhou, H. Li, N. Si, H. Li, H. Fuchs, and T. Niu, Adv. Funct. Mater. **31**, 2006997 (2021).
[13] L. Gao, J. R. Guest, and N. P. Guisinger, Nano Lett. **10**, 3512 (2010).
[14] G. E. Wood, A. J. Marsden, J. J. Mudd, M. Walker, M. Asensio, J. Avila, K. Chen, G. R. Bell, and N. R. Wilson, 2D Mater. **2**, 025003 (2015).
[15] B. Kiraly, E. V. Iski, A. J. Mannix, B. L. Fisher, M. C. Hersam, and N. P. Guisinger, Nat. Commun. **4**, 2804 (2013).
[16] F. Müller, S. Hüfner, H. Sachdev, R. Laskowski, P. Blaha, and K. Schwarz, Phys. Rev. B **82**, 113406 (2010).
[17] J. M. Wofford, E. Starodub, A. L. Walter, S. Nie, A. Bostwick, N. C. Bartelt, K. Thürmer, E. Rotenberg, K. F. McCarty, and O. D. Dubon, New J. Phys. **14**, 053008 (2012).
[18] L. Camilli, E. Sutter, and P. Sutter, 2D Mater. **1**, 025003 (2014).
[19] P. Vishnoi, K. Pramoda, and C. Rao, ChemNanoMat **5**, 1062 (2019).
[20] J. Dong, L. Zhang, X. Dai, and F. Ding, Nat. Commun. **11**, 5862 (2020).
[21] J. Gao, G. Zhang, and Y.-W. Zhang, J. Am. Chem. Soc. **138**, 4763 (2016).
[22] S. Yang, Z. Hu, W. Wang, P. Cheng, L. Chen, and K. Wu, Chin. Phys. Lett. **37**, 096803 (2020).
[23] H. Tian, J.-Q. Zhang, W. Ho, J.-P. Xu, B. Xia, Y. Xia, J. Fan, H. Xu, M. Xie, and S. Tong, Matter **2**, 111 (2020).
[24] D. Hashemi, G. Siegel, M. Snure, and S. C. Badescu, Appl. Phys. Lett. **115**, 113104 (2019).
[25] B. Feng, B. Fu, S. Kasamatsu, S. Ito, P. Cheng, C.-C. Liu, Y. Feng, S. Wu, S. K. Mahatha, P. Sheverdyaeva *et al.*, Nat. Commun. **8**, 1007 (2017).
[26] L. Tang, F. Li, and Q. Guo, Appl. Surf. Sci. **258**, 1109 (2011).
[27] N. Si and T. Niu, Nano Today **30**, 100805 (2020).
[28] G. Kresse and J. Furthmüller, Phys. Rev. B **54**, 11169 (1996).
[29] G. Kresse and J. Furthmüller, Comput. Mater. Sci. **6**, 15 (1996).
[30] P. E. Blöchl, Phys. Rev. B **50**, 17953 (1994).
[31] S. Grimme, J. Antony, S. Ehrlich, and H. Krieg, J. Chem. Phys. **132**, 154104 (2010).
[32] K. Momma and F. Izumi, J. Appl. Crystallogr. **44**, 1272 (2011).
[33] C.-C. He, S.-B. Qiu, J.-S. Yu, J.-H. Liao, Y.-J. Zhao, and X.-B. Yang, J. Phys. Chem. A **124**, 4506 (2020).
[34] C.-C. He, J.-H. Liao, S.-B. Qiu, Y.-J. Zhao, and X.-B. Yang, Comput. Mater. Sci. **193**, 110386 (2021).
[35] J. Zeng, P. Cui, and Z. Zhang, Phys. Rev. Lett. **118**, 046101 (2017).
[36] See Supplemental Material at http://link.aps.org/supplemental/10.1103/PhysRevMaterials.6.064011 for the structural details, nucleation, and growth process of blue-P on the Ag_2Sb surface alloy in the early stages.
[37] P. Sutter, J. T. Sadowski, and E. Sutter, Phys. Rev. B **80**, 245411 (2009).
[38] B. Kiraly, X. Liu, L. Wang, Z. Zhang, A. J. Mannix, B. L. Fisher, B. I. Yakobson, M. C. Hersam, and N. P. Guisinger, ACS Nano **13**, 3816 (2019).
[39] R. Wu, I. K. Drozdov, S. Eltinge, P. Zahl, S. Ismail-Beigi, I. Božović, and A. Gozar, Nat. Nanotechnol. **14**, 44 (2019).
[40] W. Li, L. Kong, C. Chen, J. Gou, S. Sheng, W. Zhang, H. Li, L. Chen, P. Cheng, and K. Wu, Sci. Bull. **63**, 282 (2018).
[41] W. Wang, H. M. Sohail, J. R. Osiecki, and R. I. G. Uhrberg, Phys. Rev. B **89**, 125410 (2014).

[42] J. Shah, W. Wang, H. M. Sohail, and R. I. G. Uhrberg, Phys. Rev. B **104**, 125408 (2021).
[43] C. R. Ast, J. Henk, A. Ernst, L. Moreschini, M. C. Falub, D. Pacilé, P. Bruno, K. Kern, and M. Grioni, Phys. Rev. Lett. **98**, 186807 (2007).
[44] J. R. Osiecki and R. I. G. Uhrberg, Phys. Rev. B **87**, 075441 (2013).
[45] E. Golias, E. Xenogiannopoulou, D. Tsoutsou, P. Tsipas, S. A. Giamini, and A. Dimoulas, Phys. Rev. B **88**, 075403 (2013).
[46] L. Moreschini, A. Bendounan, I. Gierz, C. R. Ast, H. Mirhosseini, H. Höchst, K. Kern, J. Henk, A. Ernst, S. Ostanin, F. Reinert, and M. Grioni, Phys. Rev. B **79**, 075424 (2009).
[47] Y. Girard, C. Chacon, G. de Abreu, J. Lagoute, V. Repain, and S. Rousset, Surf. Sci. **617**, 118 (2013).
[48] D. Zhou, H. Li, N. Si, Y. Jiang, H. Huang, H. Li, and T. Niu, Appl. Phys. Lett. **116**, 061602 (2020).
[49] J. Yuhara, T. Ogikubo, M. Araidai, S.-I. Takakura, M. Nakatake, and G. Le Lay, Phys. Rev. Materials **5**, 053403 (2021).
[50] W. Zhang, H. Enriquez, Y. Tong, A. J. Mayne, A. Bendounan, A. Smogunov, Y. J. Dappe, A. Kara, G. Dujardin, and H. Oughaddou, Nat. Commun. **12**, 5160 (2021).
[51] A. Schmid, N. Bartelt, and R. Hwang, Science **290**, 1561 (2000).
[52] S. Sun, T. Yang, Y. Z. Luo, J. Gou, Y. Huang, C. Gu, Z. Ma, X. Lian, S. Duan, A. T. Wee *et al.*, J. Phys. Chem. Lett. **11**, 8976 (2020).
[53] J. Jung, S. Kang, L. Nicolaï, J. Hong, J. Minár, I. Song, W. Kyung, S. Cho, B. Kim, J. D. Denlinger *et al.*, ACS Catal. **12**, 219 (2022).
[54] H. Guo, M. D. Jiménez-Sánchez, A. J. Martínez-Galera, and J. M. Gómez-Rodríguez, Adv. Mater. Interfaces **9**, 2101272 (2021).
[55] Y. Yin, V. Gladkikh, P. Li, L. Zhang, Q. Yuan, and F. Ding, Chem. Mater. **33**, 9447 (2021).
[56] S. Zhao and Z. Li, J. Phys. Chem. C **125**, 675 (2021).
[57] L. Qiu, J. Dong, and F. Ding, Nanoscale **10**, 2255 (2018).
[58] D. Muzychenko, A. Oreshkin, A. Legen'ka, and C. Van Haesendonck, Mater. Today Phys. **14**, 100241 (2020).
[59] W. Wang and R. I. G. Uhrberg, Phys. Rev. Materials **1**, 074002 (2017).
[60] L. Li, S.-z. Lu, J. Pan, Z. Qin, Y.-q. Wang, Y. Wang, G.-y. Cao, S. Du, and H.-J. Gao, Adv. Mater. **26**, 4820 (2014).
[61] H. Ding, S. S. Dwaraknath, L. Garten, P. Ndione, D. Ginley, and K. A. Persson, ACS Appl. Mater. Interfaces **8**, 13086 (2016).
[62] T. Niu, W. Zhou, D. Zhou, X. Hu, S. Zhang, K. Zhang, M. Zhou, H. Fuchs, and H. Zeng, Adv. Mater. **31**, 1902606 (2019).
[63] N. Han, N. Gao, and J. Zhao, J. Phys. Chem. C **121**, 17893 (2017).
[64] J. Zhu, C. He, Y.-H. Zhao, and B. Fu, J. Mater. Chem. C **8**, 2732 (2020).
[65] J. L. Zhang, S. Zhao, C. Han, Z. Wang, S. Zhong, S. Sun, R. Guo, X. Zhou, C. D. Gu, K. D. Yuan *et al.*, Nano Lett. **16**, 4903 (2016).
[66] J. L. Zhang, S. Zhao, S. Sun, H. Ding, J. Hu, Y. Li, Q. Xu, X. Yu, M. Telychko, J. Su *et al.*, ACS Nano **14**, 3687 (2020).
[67] D. Zhou, Q. Meng, N. Si, X. Zhou, S. Zhai, Q. Tang, Q. Ji, M. Zhou, T. Niu, and H. Fuchs, ACS Nano **14**, 2385 (2020).
[68] B. Hammer and J. Nørskov, in *Impact of Surface Science on Catalysis*, Advances in Catalysis Vol. 45 (Academic, New York, 2000), pp. 71–129.
[69] N. Mounet, M. Gibertini, P. Schwaller, D. Campi, A. Merkys, A. Marrazzo, T. Sohier, I. E. Castelli, A. Cepellotti, G. Pizzi *et al.*, Nat. Nanotechnol. **13**, 246 (2018).